

# Imprint of the anomalous magnetic moment of the $\tau$ -lepton in the $\tau^+\tau^-$ production via ultraperipheral heavy-ion collisions at the LHC.

Stefan Dittmaier\*, José Luis Hernando Ariza†, Mathieu Pellen‡

*Universität Freiburg, Physikalisches Institut,  
Hermann-Herder-Str. 3, 79104 Freiburg, Germany*

## Abstract

---

\*E-mail: stefan.dittmaier@physik.uni-freiburg.de

†E-mail: jose.luis.hernando@physik.uni-freiburg.de

‡E-mail: mathieu.pellen@physik.uni-freiburg.de

# Contents

<b>1</b>	<b>Introduction</b>	<b>1</b>
<b>2</b>	<b>Features of the calculation</b>	<b>2</b>
2.1	Equivalent-photon approximation . . . . .	2
2.2	Form-factor approach . . . . .	2
2.2.1	Form-factor decomposition of the $\gamma\bar{\tau}\tau$ vertex function . . . . .	2
2.2.2	Extracting the contribution from $a_\tau$ . . . . .	2
2.2.3	Coulomb term and Sommerfeld enhancement . . . . .	3
2.2.4	Analytical expressions for the helicity amplitudes (?) . . . . .	3
2.3	Technical aspects of the calculation and employed tools . . . . .	3
2.4	Set-up of the calculation . . . . .	3
<b>3</b>	<b>Results</b>	<b>4</b>
3.1	Determination of $a_\tau$ in UPCs . . . . .	4
3.2	Validity of the form-factor approach . . . . .	5
3.2.1	Inclusive $\tau$ -pair production . . . . .	5
3.2.2	$\tau$ -pair production in UPCs assuming leptonic $\tau$ -decays . . . . .	9
3.3	Impact of a non-zero electric dipole moment in the cross section (?) . . . . .	11
<b>4</b>	<b>Conclusion</b>	<b>11</b>

## 1 Introduction

## 2 Features of the calculation

### 2.1 Equivalent-photon approximation

- Describe the EPA (as in the previous paper).

### 2.2 Form-factor approach

- Keep this section for a general lepton and focus on the  $\tau$ -lepton in the numerics to emphasize that the same analysis can be done for  $e$  and  $\mu$  as a check of the method(?)

#### 2.2.1 Form-factor decomposition of the $\gamma\bar{\tau}\tau$ vertex function

- Mention the problem of the off-shell  $\tau$  in the standard approach.
  - Outline the way how the general form-factor decomposition is obtained.
  - Give the general form-factor decomposition in the on-shell basis.

[JH: Change the structures to  $\Lambda_+(\bar{p}) \pm \Lambda_-(p)$  and adapt table.]

$$\begin{aligned} \Gamma_\mu^{\gamma\bar{f}f}(k, \bar{p}, p) = e & \left[ \gamma_\mu g_1 + \gamma_\mu \gamma_5 g_2 + \frac{i\sigma_{\mu\nu} k^\nu}{2m} g_3 + \frac{\sigma_{\mu\nu} \gamma_5 k^\nu}{2m} g_4 + \frac{ik_\mu}{2m} g_5 + \frac{k_\mu}{2m} \gamma_5 g_6 \right. \\ & + \Lambda_+(\bar{p}) \gamma_\mu g_7 + \Lambda_+(\bar{p}) \gamma_\mu \gamma_5 g_8 + \frac{\bar{k}_\mu}{2m} \Lambda_+(\bar{p}) g_9 + \frac{i\bar{k}_\mu}{2m} \Lambda_+(\bar{p}) \gamma_5 g_{10} \\ & + \frac{ik_\mu}{2m} \Lambda_+(\bar{p}) g_{11} + \frac{k_\mu}{2m} \Lambda_+(\bar{p}) \gamma_5 g_{12} \\ & + \gamma_\mu \Lambda_-(p) g_{13} + \gamma_\mu \gamma_5 \Lambda_-(p) g_{14} + \frac{\bar{k}_\mu}{2m} \Lambda_-(p) g_{15} + \frac{i\bar{k}_\mu}{2m} \gamma_5 \Lambda_-(p) g_{16} \\ & + \frac{ik_\mu}{2m} \Lambda_-(p) g_{17} + \frac{k_\mu}{2m} \gamma_5 \Lambda_-(p) g_{18} \\ & + \Lambda_+(\bar{p}) \gamma_\mu \Lambda_-(p) g_{19} + \Lambda_+(\bar{p}) \gamma_\mu \gamma_5 \Lambda_-(p) g_{20} \\ & + \frac{\bar{k}_\mu}{2m} \Lambda_+(\bar{p}) \Lambda_-(p) g_{21} + \frac{i\bar{k}_\mu}{2m} \Lambda_+(\bar{p}) \gamma_5 \Lambda_-(p) g_{22} \\ & \left. + \frac{ik_\mu}{2m} \Lambda_+(\bar{p}) \Lambda_-(p) g_{23} + \frac{k_\mu}{2m} \Lambda_+(\bar{p}) \gamma_5 \Lambda_-(p) g_{24} \right], \end{aligned} \quad (1)$$

- Give the from-factor decomposition in the standard kinetical configuration and in “ours”.

- Remark that the decomposition is gauge dependent (Ward identities).

#### 2.2.2 Extracting the contribution from $a_\tau$

- Write matrix element with the general vertex decomposition.
  - Perform an expansion of the form factors in  $\alpha$ .
  - Remark again the presence of gauge dependence in this decomposition.
  - Remark the absence of effects due to real radiation in the form factor approach.
  - Perform Taylor expansion of the form factors around  $\frac{x}{s} \sim \frac{m^2}{s}$  ( $x = t, u$ ) to extract  $a_\tau$  and  $d_\tau$  contributions.

Space-time symmetry	$\mathcal{P}$	$\mathcal{C}$	$\mathcal{T}$	$\mathcal{CP}$	$\mathcal{CPT}$
$g_1, g_3, g_7, g_9, g_{13}, g_{15}, g_{19}, g_{21}$	✓	✓	✓	✓	✓
$g_2, g_8, g_{14}, g_{20}$	✗	✗	✓	✓	✓
$g_4, g_{10}, g_{16}, g_{22}$	✗	✓	✗	✗	✓
$g_5, g_{11}, g_{17}, g_{23}$	✓	✗	✗	✗	✓
$g_6, g_{12}, g_{18}, g_{24}$	✗	✗	✓	✓	✓

Table 1: Summary of the preserved/violated space-time symmetries by the covariant structures associated with each form factor  $g_i$ . The symbols ✓ and ✗ indicate if the space-time symmetry is preserved or violated, respectively.

### 2.2.3 Coulomb term and Sommerfeld enhancement

- Explain the need of including the Coulomb term.
  - Give the contribution from Coulomb term.

### 2.2.4 Analytical expressions for the helicity amplitudes (?)

- Give analytical expression in the spinor-helicity formalism for  $\mathcal{M}^{(0)}$ ,  $\mathcal{M}^{a_\tau}$ ,  $\mathcal{M}^{d_\tau}$ .

## 2.3 Technical aspects of the calculation and employed tools

- Comment the use of equivalent-photon approximation and GAMMA-UPC.
  - Comment the use of the ChFF to parameterize the photon flux.
  - Comment the use of iNWA to include spin correlations.
  - Comment the use of mixed input-parameter scheme.

### Remarks about the NLO prediction (?)

- Reference to the previous paper for details on the NLO corrections.
  - Mention the gauge invariant splitting of the NLO corrections.

### Checks on the calculation (?)

- Analytical expressions checked against FeynArts.
  - Correct behaviour under  $\mathcal{P}$ ,  $\mathcal{C}$  and  $\mathcal{CP}$  of  $\mathcal{M}^{(0)}$ ,  $\mathcal{M}^{a_\tau}$ ,  $\mathcal{M}^{d_\tau}$  (?).

## 2.4 Set-up of the calculation

### Numerical input

- Numerical inputs

### Event selection (?)

- ATLAS set-up

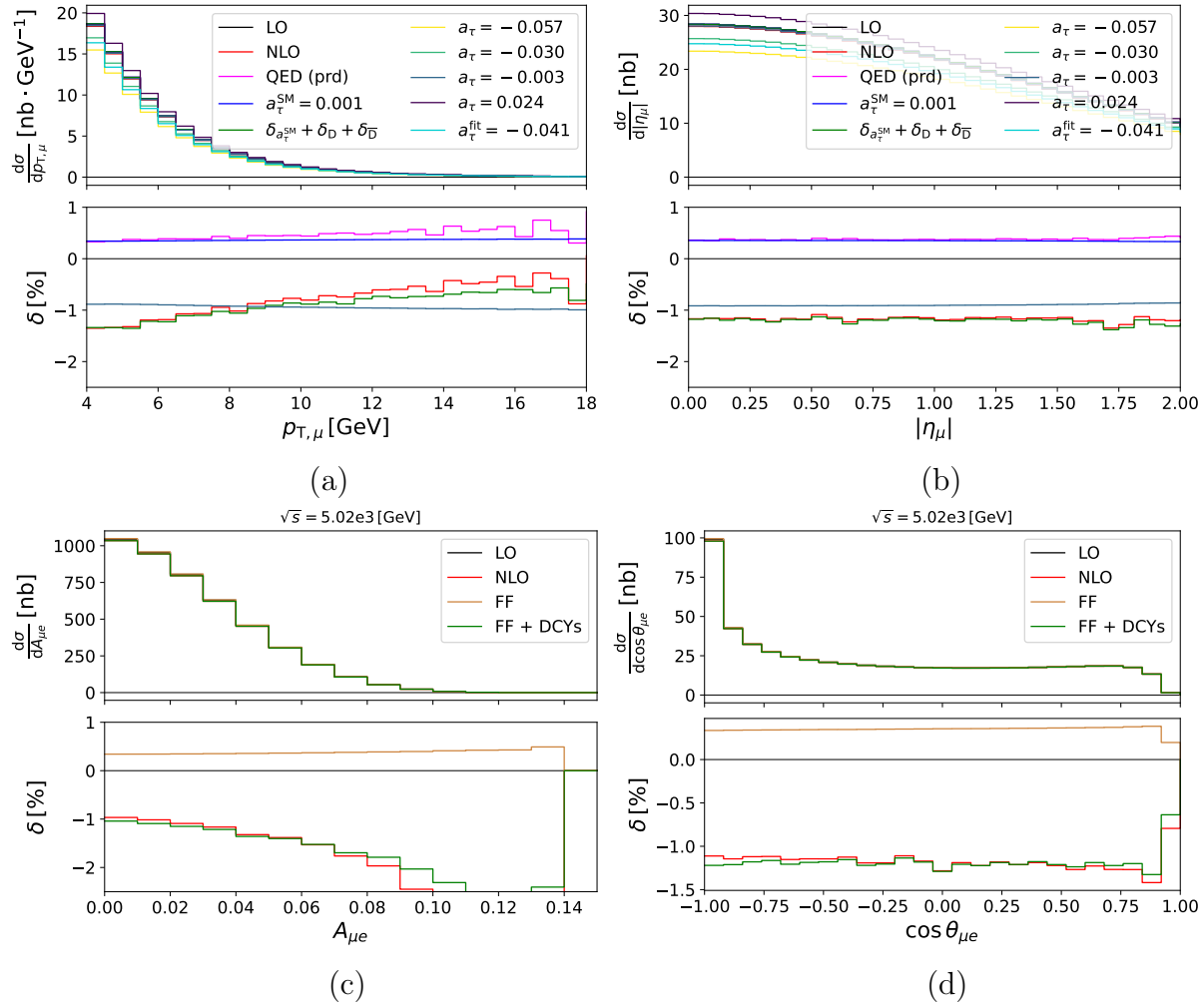


Figure 1: Predictions for  $\gamma\gamma \rightarrow \tau^+\tau^- \rightarrow e^+\mu^-\bar{\nu}_\tau\nu_\tau\bar{\nu}_\mu\nu_e$  induced by UPCs of two lead ions with  $\sqrt{s_{\text{PbPb}}} = 5.02$  TeV. The panels (a) and (b) show predictions for the transverse momentum and the pseudorapidity of  $\mu^-$ , and the panels (c) and (d) provide predictions for the acoplanarity and the angle between  $\mu^-$  and  $e^+$ , respectively. **The different curves show ....** The lower panel gives the relative correction  $\delta^i = \frac{\Delta\sigma^i}{\sigma^{\text{LO}}}$ .

[JH: Show plots like the upper panels or like the lower panels?. I prefer the upper ones, but maybe for less  $a_\tau$ -values ( $a_\tau = -0.057, -0.003, 0.001, 0.024$ ) and remove QED (prd).]

### 3 Results

#### 3.1 Determination of $a_\tau$ in UPCs

- Show the comparison between  $\sigma^{\text{NLO}}$  vs  $\sigma^{\text{FF}}$  in the ATLAS set-up.
- Remark the importance of including corrections to the  $\tau$ -decays in the form-factor calculation. Specially if  $p_{T,\mu}$  is employed.
- Recall the importance of the photon-flux parametrization.
- Recall the importance of including spin correlations between the produced  $\tau$ -leptons.

$\sqrt{s_{\gamma\gamma}}$ [GeV]	$\sigma^{\text{LO}}$ [nb]	$\delta^{\text{QED}} [\%]$	$\delta^{a_\tau} [\%]$	$\delta^{\text{Coul.}} [\%]$	$\delta^{\text{FF}} [\%]$	$\Delta_{\text{FF}} [\%]$
3.8	7.9548(1)	2.6853(4)	0.3901(1)	2.4757(1)	2.8658(1)	0.1804(4)
5	14.065(1)	0.7933(1)	0.3009(1)	0.4158(1)	0.7167(1)	-0.0765(1)
10	7.1323(1)	0.3857(1)	0.2876(1)	0.0196(1)	0.3072(1)	-0.0785(1)
18	3.0310(1)	0.6996(2)	0.2842(1)	0.0018(1)	0.2856(1)	-0.4136(2)

Table 2: Inclusive cross-section for  $\gamma\gamma \rightarrow \tau^+\tau^-$  for different fixed photon–photon centre-of-mass energies, which are indicated in the first column. The second column gives the LO cross section. The third column provides the QED relative correction. The fourth and fifth columns correspond to the relative corrections from the anomalous magnetic moment and from the Coulomb term, respectively. The sixth column gives the total relative correction in the form-factor approach. Finally, the last column correspond to the difference between the NLO QED relative correction and the form-factor relative correction.

### 3.2 Validity of the form-factor approach

- Show the relevance of the non-included effects in the form-factor approach, *i.e.*

$$\Delta_{\text{FF}} = \frac{\sigma^{\text{FF}} - \sigma_P^{\text{QED}}}{\sigma_P^{\text{QED}}} \quad (2)$$

- Show  $\frac{t-m^2}{s}$  (?) at LO (?) at NLO (?).

#### 3.2.1 Inclusive $\tau$ -pair production

- Comparison just for the production, *i.e.* no  $\tau$ -decays.
  - Show it just for unpolarized  $\tau$ -leptons.
  - Remark that  $a_\tau$  is part of QED corrections, which are gauge invariant independently and, thus, they can be compared.

#### Fixed photon–photon centre-of-mass energy

- Show comparison for fixed c.m.e. (3.8, 5, 10, 18 GeV? or all?)
- Remark importance of the Coulomb term for small c.m.e..
- Remark the importance of using observables that are not sensitive to collinear radiation off the produced  $\tau$ -leptons.

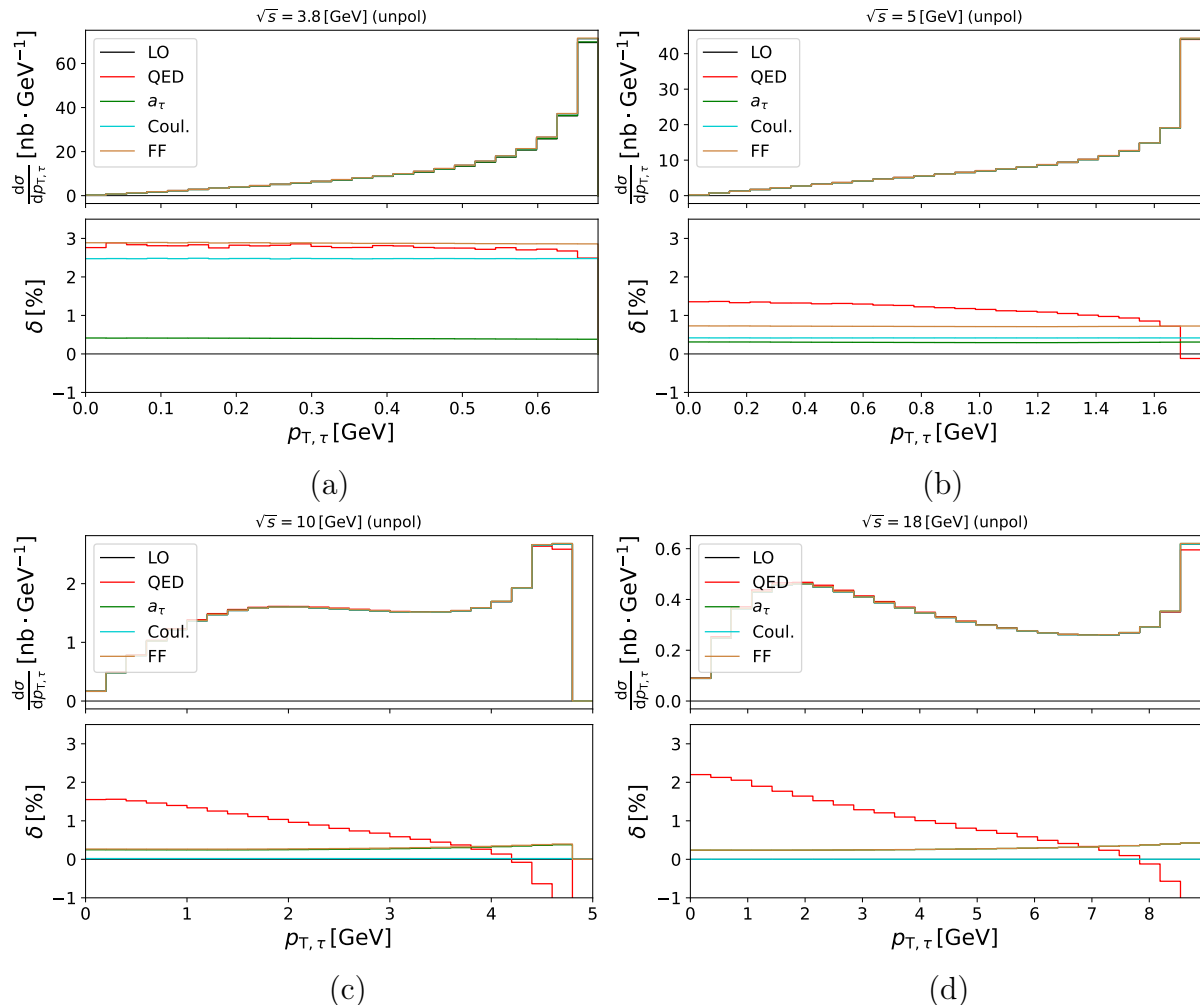


Figure 2: Predictions for  $\gamma\gamma \rightarrow \tau^+\tau^-$  for different photon–photon centre-of-mass energies: (a)  $\sqrt{s_{\gamma\gamma}} = 3.8$  GeV, (b)  $\sqrt{s_{\gamma\gamma}} = 5$  GeV, (c)  $\sqrt{s_{\gamma\gamma}} = 10$  GeV, and (d)  $\sqrt{s_{\gamma\gamma}} = 18$  GeV. The different curves show the transverse momentum of the  $\tau^-$ -lepton at LO (black) and including NLO QED correction (red), the contribution from the anomalous magnetic moment (green), the contribution from the Coulomb term (blue), and the total correction obtained in form-factor approach (brown). The lower panel gives the relative correction  $\delta^i = \frac{\Delta\sigma^i}{\sigma^{\text{LO}}}$ .

[JH: Remove (unpol.) in title and add subscript  $\gamma\gamma$ .]

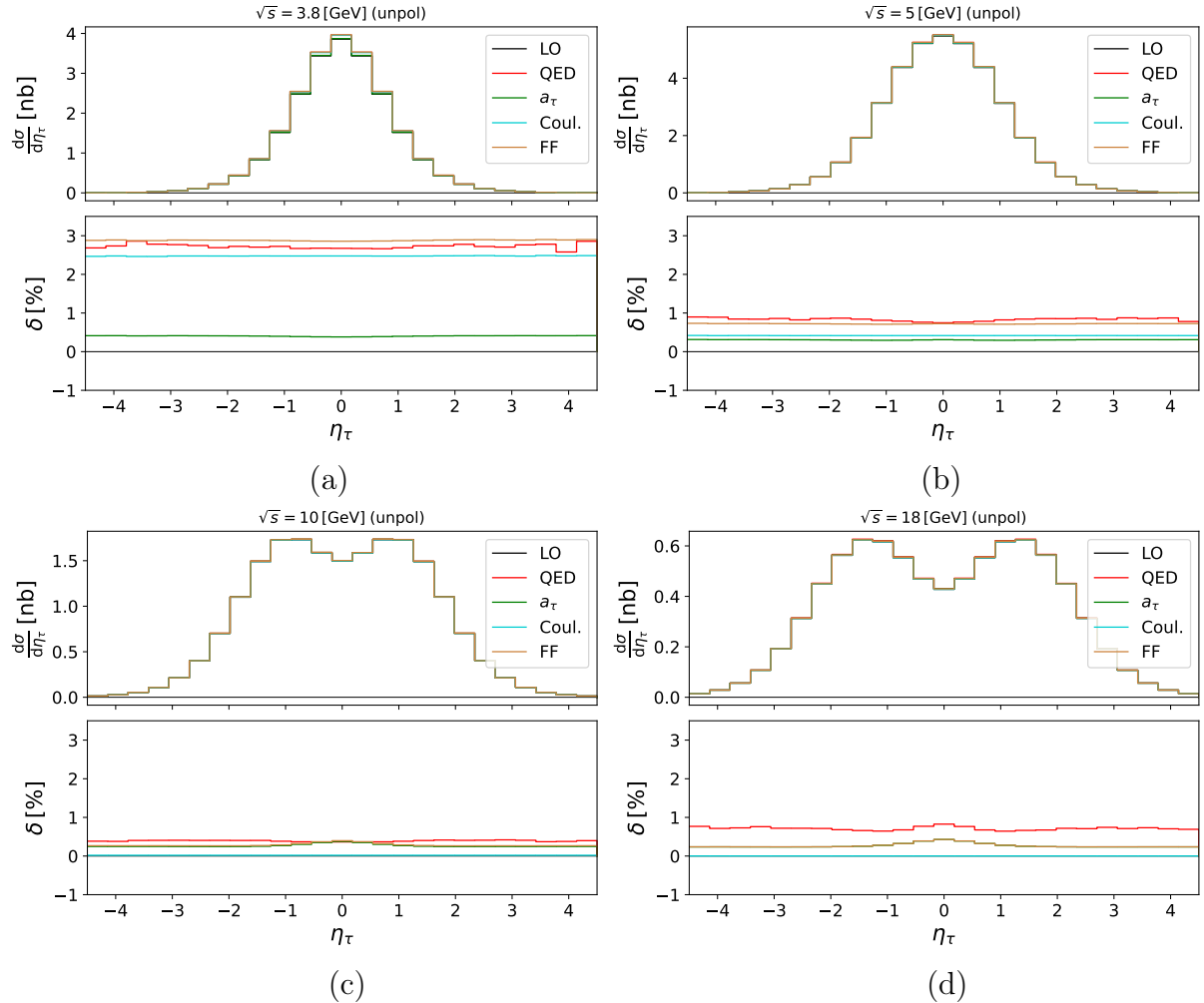


Figure 3: Same as Fig. 2, but for the pseudorapidity of the  $\tau^-$ -lepton.

[JH: Change to  $|\eta_\tau|$  and more bins.]

[JH: Remove (unpol.) in title and add subscript  $\gamma\gamma$ .]

$\sigma^{\text{LO}} [\text{mb}]$	$\delta^{\text{QED}} [\%]$	$\delta^{a_\tau} [\%]$	$\delta^{\text{Coul.}} [\%]$	$\delta^{\text{FF}} [\%]$	$\Delta_{\text{FF}} [\%]$
1.0617(1)	0.945(1)	0.308(1)	0.589(1)	0.898(1)	-0.047(1)

Table 3: Inclusive cross-section for  $\gamma\gamma \rightarrow \tau^+\tau^-$  induced by UPCs of two lead ions with  $\sqrt{s_{\text{PbPb}}} = 5.02 \text{ TeV}$ . The first column gives the LO cross section. The second column provides the QED relative correction. The third and fourth columns correspond to the relative corrections from the anomalous magnetic moment and from the Coulomb term, respectively. The fifth column gives the total relative correction in the form-factor approach. Finally, the last column correspond to the difference between the NLO QED relative correction and the form-factor relative correction.

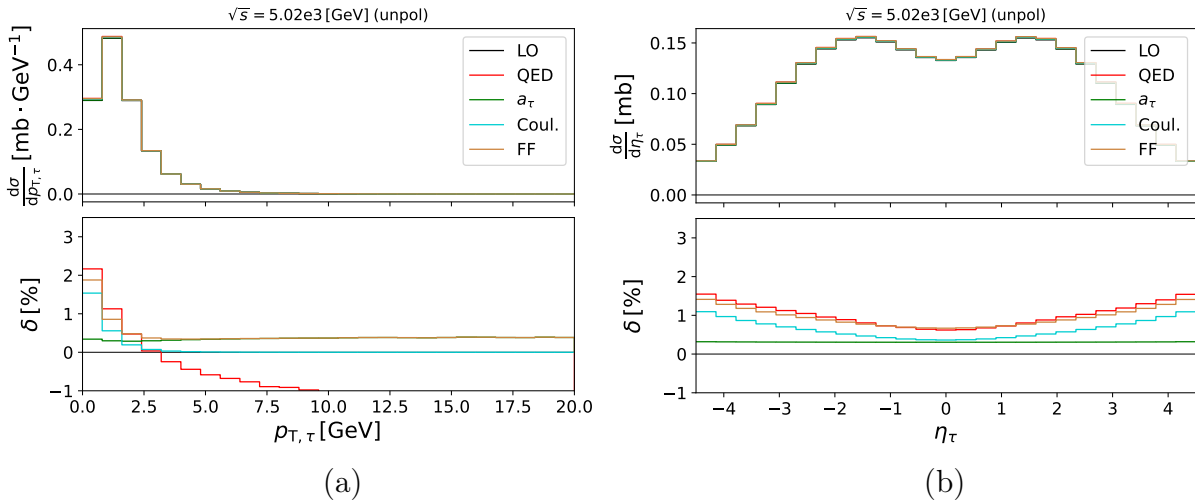


Figure 4: Inclusive cross-section for  $\gamma\gamma \rightarrow \tau^+\tau^-$  induced by UPCs of two lead ions with  $\sqrt{s_{\text{PbPb}}} = 5.02 \text{ TeV}$ . The panels (a) and (b) show the prediction for the transverse momentum and the pseudorapidity of the  $\tau^-$ -lepton, respectively. The different curves show prediction at LO (black) and including NLO QED correction (red), the contribution from the anomalous magnetic moment (green), the contribution from the Coulomb term (blue), and the total correction obtained in form-factor approach (brown). The lower panel gives the relative correction  $\delta^i = \frac{\Delta\sigma^i}{\sigma^{\text{LO}}}$ .

[JH: Change (b) to  $|\eta_\tau|$  and more bins.]

[JH: Remove title.]

## Ultraperipheral heavy-ion collision

- Show comparison with photon flux.
  - Mention the problem in Ref. [1]:
  - \* Wrong input-parameter scheme → Fixable by considering the cross section, not just the correction.
  - \* They do not include the Coulomb term → Wrong value for  $a_\tau$  obtained.

cuts	$\sigma^{\text{LO}} [\text{nb}]$	$\delta^{\text{QED}} [\%]$	$\delta^{a_\tau} [\%]$	$\delta^{\text{Coul.}} [\%]$	$\delta^{\text{FF}} [\%]$	$\Delta_{\text{FF}} [\%]$
Inclusive	32920(3)	0.9440(7)	0.3084(1)	0.5893(1)	0.8976(1)	-0.046(1)
$p_{\text{T},\ell} > 4 \text{ GeV}$ $ \eta_\ell  < 2.5$	45.877(7)	0.3792(8)	0.3483(1)	0.0017(1)	0.3500(1)	-0.029(1)
$p_{\text{T},\ell} > 2 \text{ GeV}$ $ \eta_\ell  < 2.5$	438.22(6)	0.3021(5)	0.3310(1)	0.0180(1)	0.3490(1)	0.047(1)
$p_{\text{T},\ell} > 6 \text{ GeV}$ $ \eta_\ell  < 2.5$	10.137(2)	0.456(2)	0.3531(1)	0.0004(1)	0.3535(1)	-0.102(1)
$p_{\text{T},\ell} > 4 \text{ GeV}$ $ \eta_\ell  < 3.5$	49.911(8)	0.3845(8)	0.3445(1)	0.0017(1)	0.3463(1)	-0.038(1)
$p_{\text{T},\ell} > 4 \text{ GeV}$ $ \eta_\ell  < 2$	39.237(6)	0.371(1)	0.3532(1)	0.0017(1)	0.3549(1)	-0.016(1)

Table 4: Cross section for  $\gamma\gamma \rightarrow \tau^+\tau^- \rightarrow e^+\mu^-\bar{\nu}_\tau\nu_\tau\bar{\nu}_\mu\nu_e$  induced by UPCs of two lead ions with  $\sqrt{s_{\text{PbPb}}} = 5.02 \text{ TeV}$  for different cut configurations.

[JH: Change.]

### 3.2.2 $\tau$ -pair production in UPCs assuming leptonic $\tau$ -decays

- Comparison including leptonic  $\tau$ -decays.
- Show the comparison between  $\sigma_{\text{P}}^{\text{QED}}$  vs  $\sigma^{\text{FF}}$ .
- Remark that the corrections to the production are gauge invariant by their own and, thus, can be compared to determine  $\Delta_{\text{FF}}$ .

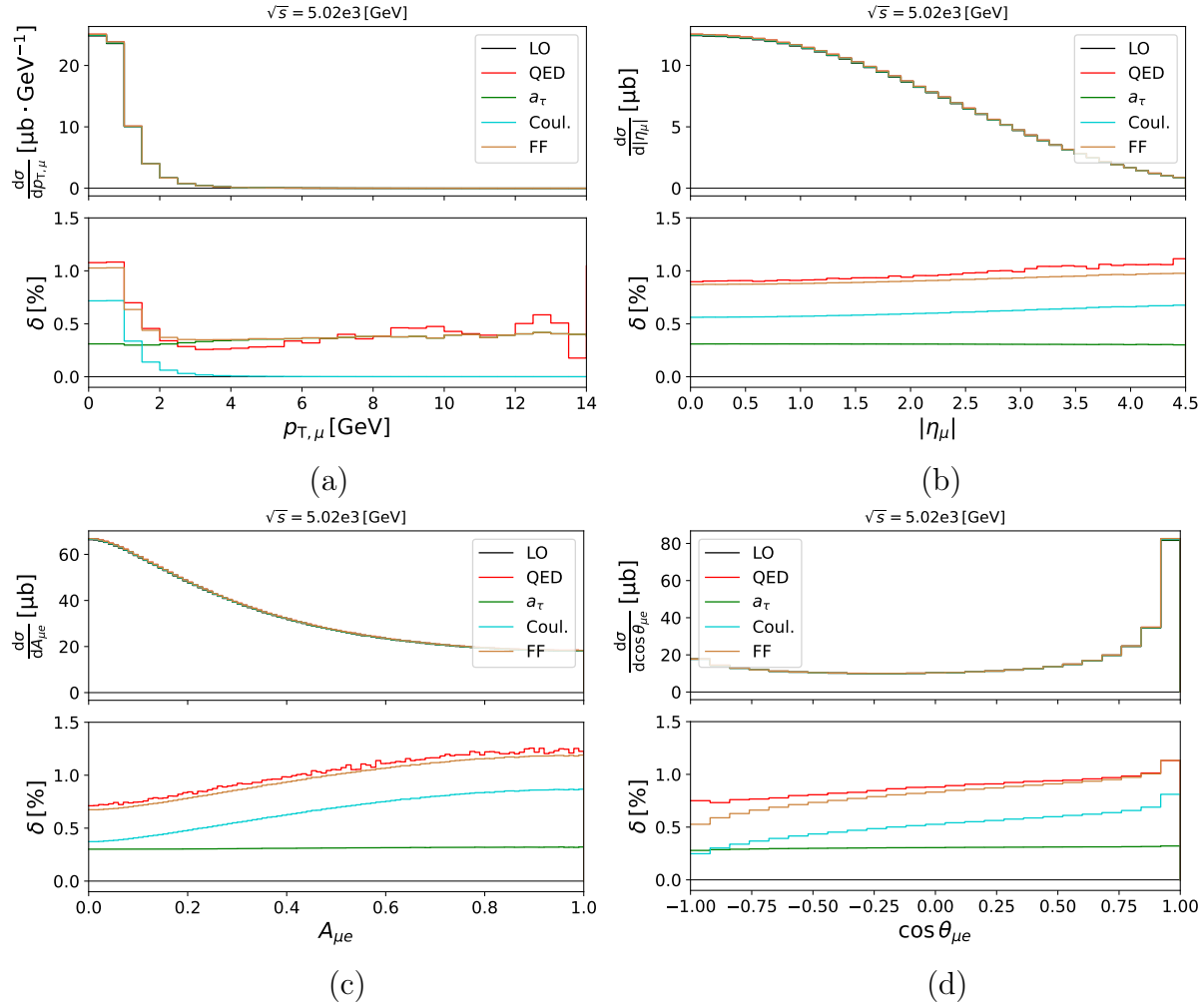


Figure 5: Predictions for  $\gamma\gamma \rightarrow \tau^+\tau^- \rightarrow e^+\mu^-\bar{\nu}_\tau\nu_\tau\bar{\nu}_\mu\nu_e$  induced by UPCs of two lead ions with  $\sqrt{s_{\text{PbPb}}} = 5.02$  TeV. The panels (a) and (b) show predictions for the transverse momentum and the pseudorapidity of  $\mu^-$ , and the panels (c) and (d) provide predictions for the acoplanarity and the angle between  $\mu^-$  and  $e^+$ , respectively. The different curves show the transverse momentum of the  $\tau^-$ -lepton at LO (black) and including NLO QED correction (red), the contribution from the anomalous magnetic moment (green), the contribution from the Coulomb term (blue), and the total correction obtained in form-factor approach (brown). The lower panel gives the relative correction  $\delta^i = \frac{\Delta\sigma^i}{\sigma^{\text{LO}}}$ .

[JH: Remove title.]

### Dependence on the choice of $p_{T,\ell}$ cuts

- Show the comparison for  $p_{T,\ell} > 2, 4, 6$  GeV and  $|\eta_\ell| < 2.5$ .
  - Add  $p_{T,\ell} > 0$  GeV and  $|\eta_\ell| < 2.5$  (?).
  - Comment the problem of having a large  $p_{T,\ell}$  cut if enough precision is reached.
  - For the plots: Do a figure for each observable and different cuts (inclusive apart) or do a figure for each cut configuration (?).

### Spin-correlation effects (?)

- I would say no, it is repetitive with the paper. I would just mention it in Sec. 3.1.

### 3.3 Impact of a non-zero electric dipole moment in the cross section (?)

- $d_\tau^{\text{SM}} = 0$ .
- $\mathcal{O}(d_\tau^{\text{BSM}}) \rightarrow 0$ .
- $\mathcal{O}((d_\tau^{\text{BSM}})^2)$  terms needed.

## 4 Conclusion

## Appendix

## References

- [1] J. Jiang, P.-C. Lu, Z.-G. Si, H. Zhang, and X.-Y. Zhang, *NLO EW corrections to tau pair production via photon fusion in Pb-Pb ultraperipheral collision.*  
[arXiv:2410.21963 \[hep-ph\]](https://arxiv.org/abs/2410.21963).